Electronic Supplementary Information (ESI)

MnV_2O_6/Graphene Nanocomposite as Efficient Electrocatalysts for the Oxygen Evolution Reaction

Kyeong-Ho Kim[1], Yun-Hyuk Choi[2,], and Seong-Hyeon Hong[1,]**

[1]Department of Materials Science and Engineering and Research Institute of Advanced Materials, Seoul National University, Seoul 151-744, Republic of Korea

[2]School of Advanced Materials and Chemical Engineering, Daegu Catholic University, Gyeongsan, Gyeongbuk 38430, Republic of Korea

* Corresponding author
Prof. Seong-Hyeon Hong (S.-H. Hong)
E-mail: shhong@snu.ac.kr
Prof. Yun-Hyuk Choi (Y.-H. Choi)
E-mail: yunhyukchoi@cu.ac.kr

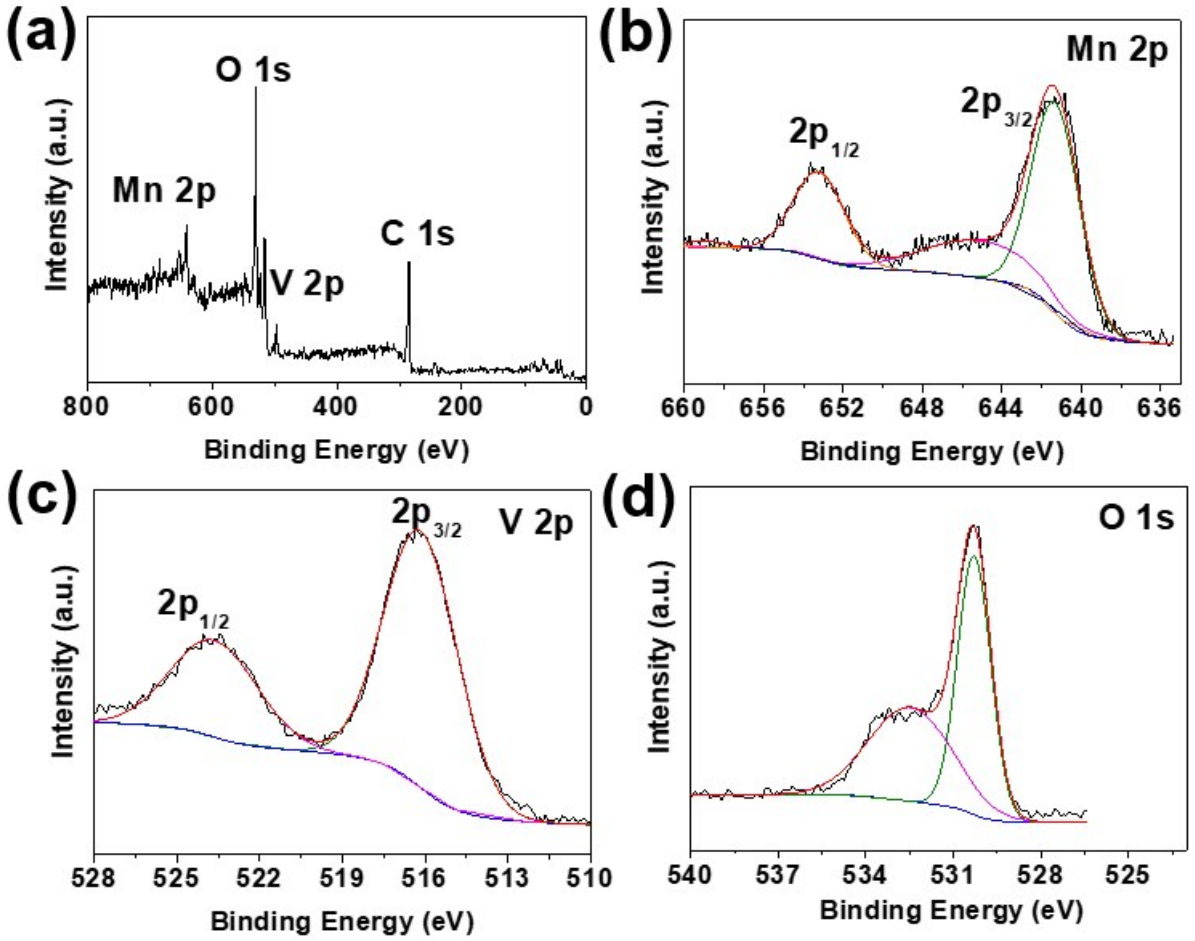

Fig. S1 XPS spectra of as-prepared MnV_2O_6 nanobelts for (a) survey, (b) Mn 2p, (c) V 2p, and (d) O 1s.

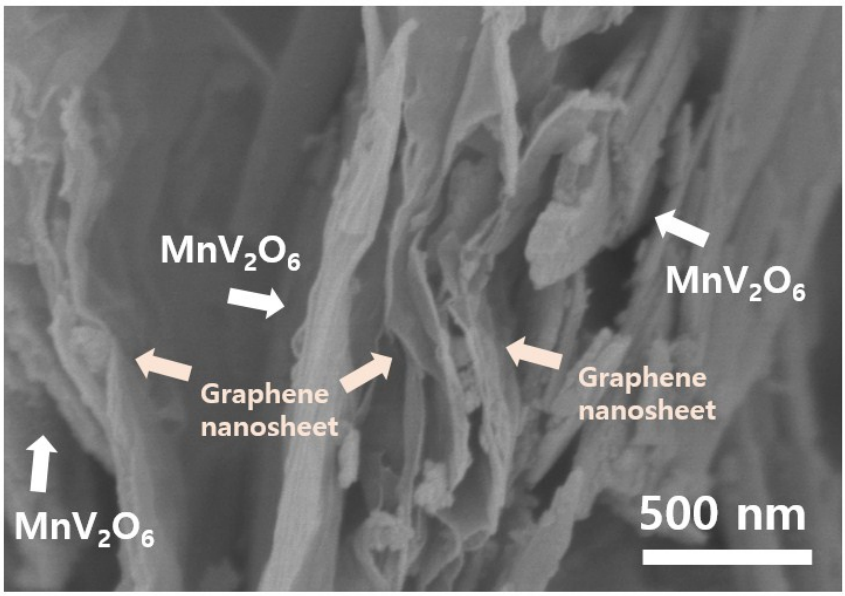

Fig. S2 High magnification SEM image of MnV_2O_6/graphene nanocomposite.

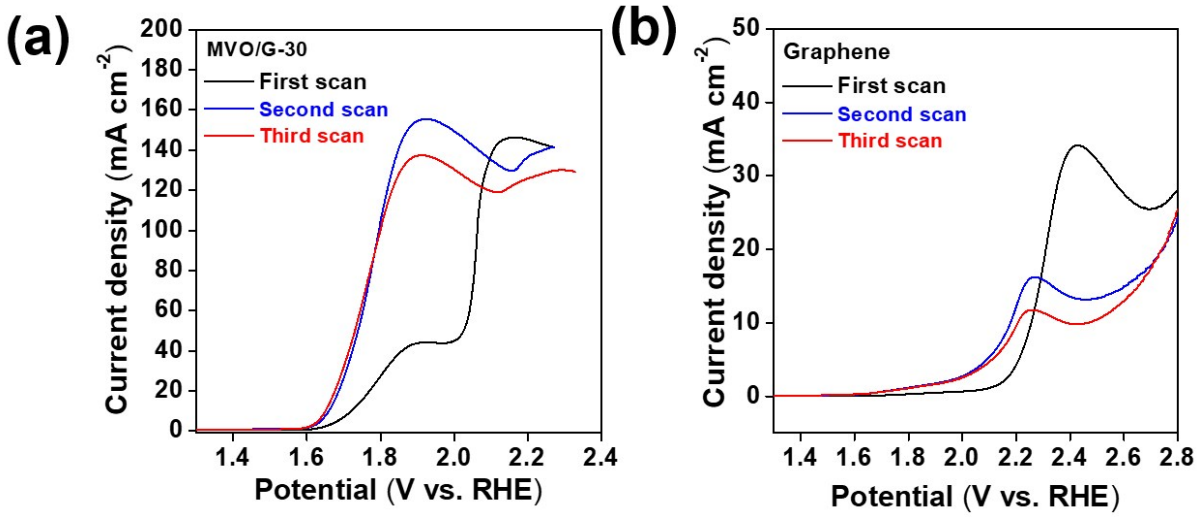

Fig. S3 Linear scan voltammogram (LSV) curves of (a) MVO/G-30 and (b) bare graphene, measured in 1 M KOH aqueous solution.

Table S1 OER performance comparison of MnV_2O_6/graphene nanocomposite with the previously reported transition metal oxide/carbon nanocomposites for OER electrocatalysts.

OER catalyst	OER performance				
	[KOH] (M)	I (mA cm^{-2})	η (mV)	Tafel slop (mV dec^{-1})	Ref.
IrO_2	1	10	330	76	[1]
V-Co/CoO@C	1	10	320	143	[2]
Co-Fe-O/rGO	1	10	340	31	[3]
Co_3O_4/BCN	1	10	394	-	[4]
MnV_2O_6/G	1	10	396	66	This work
$CuCo_2O_4$/NrGO	0.1	10	410	-	[5]
Mn_3O_4/CNT	1	10	410	-	[6]
$Mn_{1.5}V_{1.5}O_4$/NrGO	0.1	10	420	271	[7]
$Mn_2V_2O_7$/NrGO	0.1	10	440	286	[7]
Pt-Mn_3O_4/C	0.1	1.4	470	-	[8]
Pt-Mn_3O_4/CB@graphite	0.1	5	470	63	[9]
Mn_3O_4@G	1	10	473	85	[10]
$CoFe_2O_4$/rGO	0.1	10	540	-	[11]
Mn_3O_4@glassy carbon	0.1	8.36	570	71.5	[12]
MnO_2/C	0.1	10	570	-	[13]
MnO_2@Pd@C	1	2.6	700	-	[14]

[1] Zhang, J. et al. *Angew. Chem.*, 2016, **128**, 6814–6819.

[2] Huang, H. et al. *Inorg. Chem., Commun.*, 2019, **103**, 1–5.

[3] Geng, J. et al. *Chem. Sus. Chem.*, 2015, **4**, 659-664.

[4] Balakrishnan, T. et al. *RSC Adv.,* 2016, **6**, 79448–79451.

[5] Bikkarolla, S. K. et al. *J. Power Sources*, 2015, **281**, 243-251.

[6] Li, L. et al. *ACS Appl. Energy Mater.*, 2018, **1**, 963–969.

[7] Xing, X. et al. *ACS Appl. Mater. Interfaces*, 2018, **10**, 44511-44517.

[8] Li, Z.-Y. et al. *Electrochim. Acta*, 2014, **146**, 119–124.

[9] Li, Z.-Y. et al. *J. Mater. Chem. A,* 2014, **2**, 18236–18240.

[10] Li, M. et al. *Int. J. Hydrogen Energy*, 2018, **43**, 15807–15814.

[11] Godinho, M. I. et al. *Electrochim. Acta*, 2003, **47**, 4307–4314.

[12] Guo, C. X. et al. *Nanoscale*, 2014, **6**, 10896–10901.

[13] Kim, H.-M. et al. *ChemistrySelect*, 2018, **3**, 6302–6308.

[14] Zhang, J.-H. et al. *Electrochim. Acta*, 2016, **196**, 661–669.

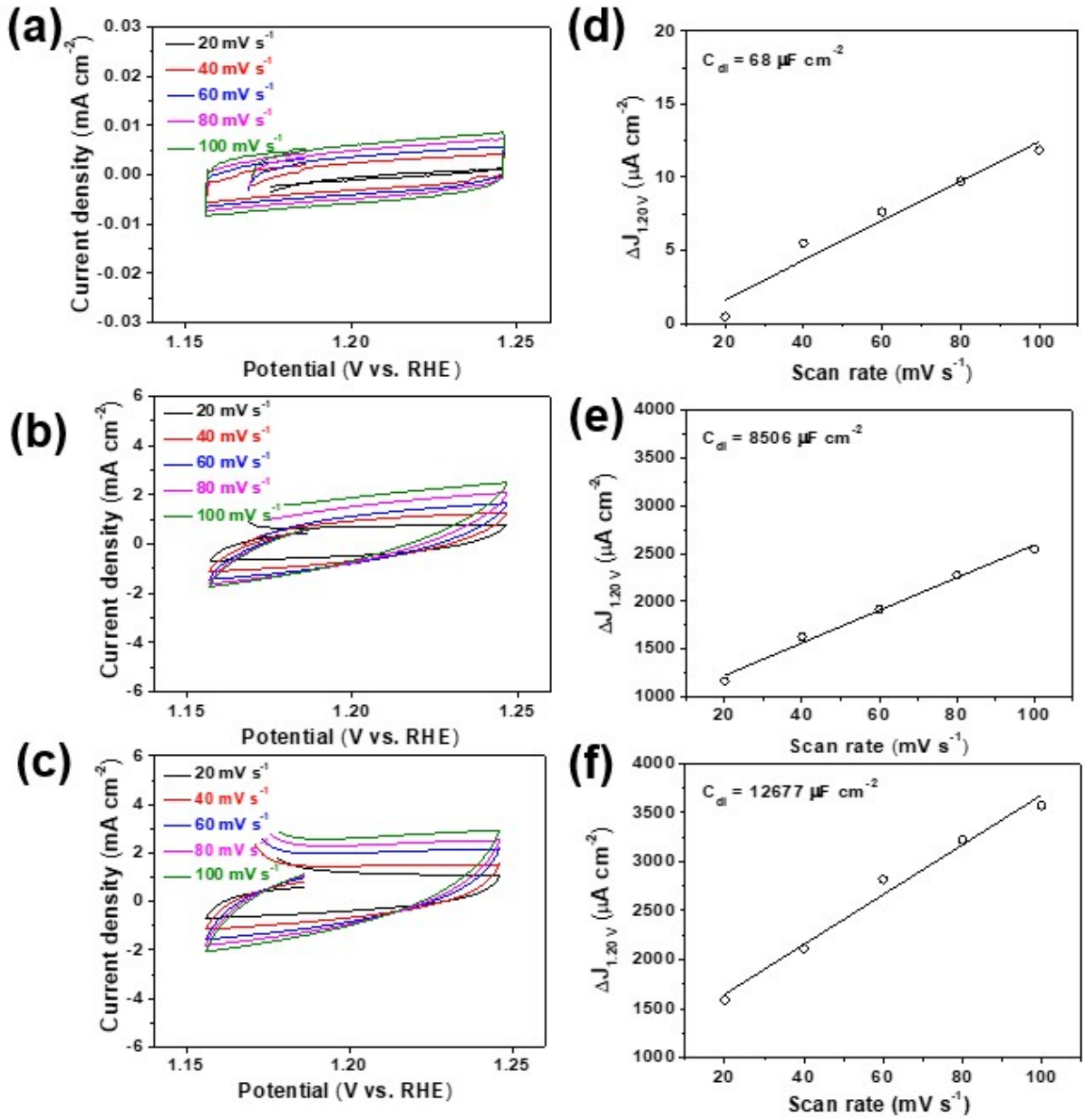

Fig. S4 Cyclic voltammograms acquired at scan rates of 20-100 mV s^{-1} in the range of 1.156-1.246 V *versus* RHE for (a) MVO, (b) MVO/G-10, and (c) MVO/G-20. (d-f) The differences (ΔJ) of anodic and cathodic current densities at 1.20 V *versus* RHE (in the non-Faradaic region) plotted as a function of the scan rate. Each plot is fitted to a straight line to determine the C_{dl} values.

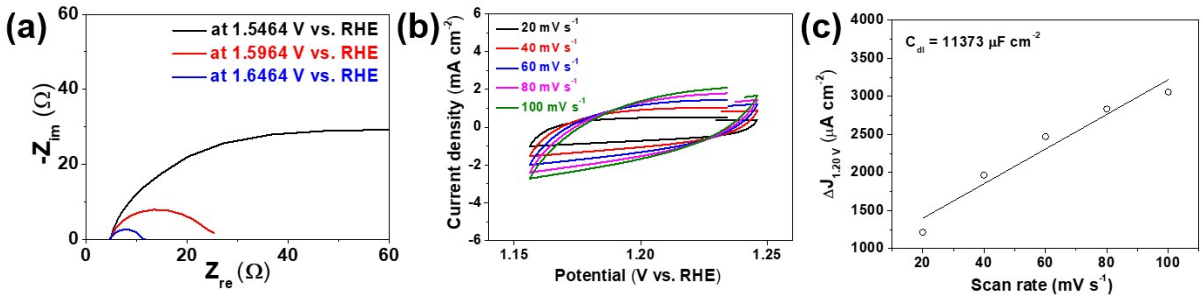

Fig S5. (a) Nyquist plots measured at 1.5464, 1.5964, and 1.6464 V vs. RHE, (b) cyclic voltammograms, and (c) differences (ΔJ) of anodic and cathodic current densities plotted as a function of the scan rate for MVO/G-20 after 1000 CV cycles. The plot is fitted to a straight line to determine the C_{dl} value.

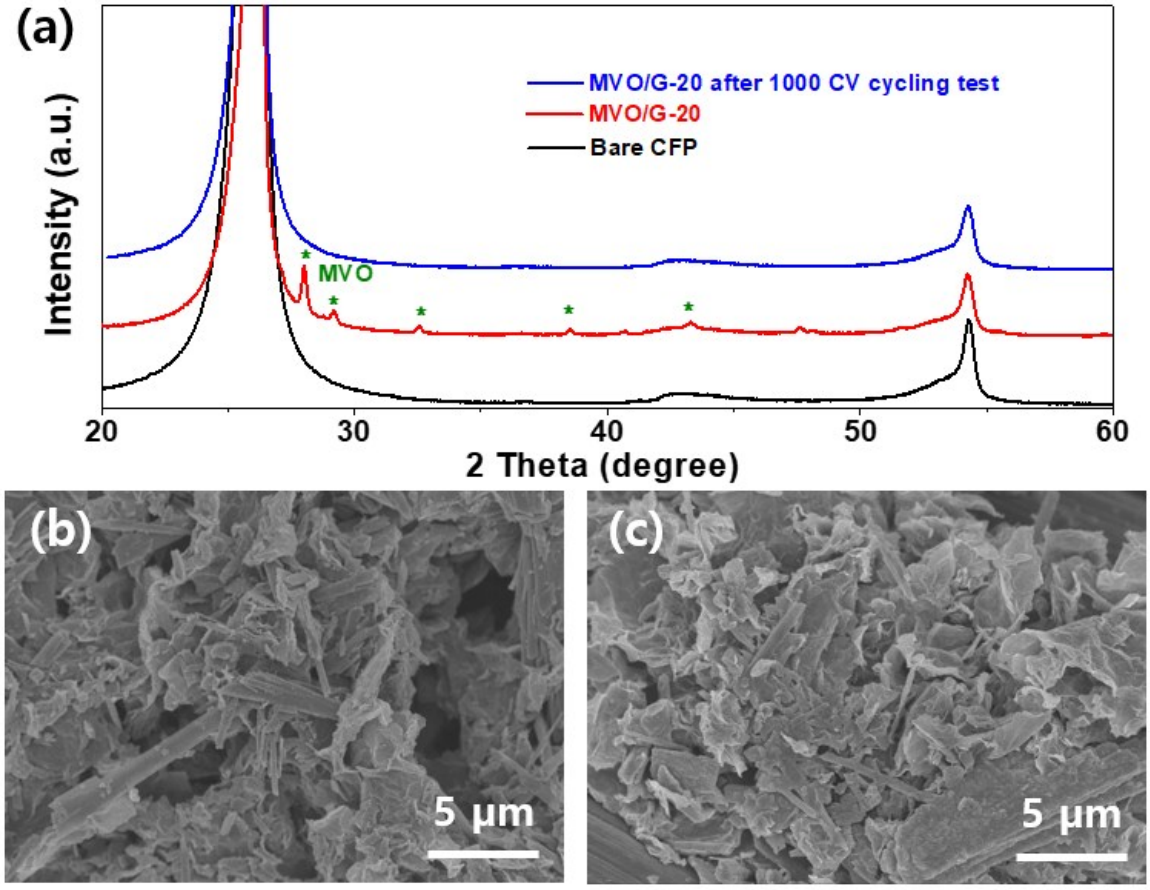

Fig. S6 (a) XRD patterns for Bare CFP, MVO/G-20, and MVO/G-20 after 1000 CV cycling test and SEM images of MVO/G-20 (b) before cycle and (c) after 1000 CV cycling test, respectively.

"As shown in the XRD patterns (Fig. S6a†), MVO became amorphous after 1000 CV cycles and this amorphization was also observed in other transition metal oxide electrocatalysts.[1-3] The morphological observation by SEM indicated that there was no significant change in the morphology of MVO/G-20 after 1000 CV cycling test (Fig. S6b-c†)."

Ref.

[1] *J. Phys. Chem. Lett.*, 2012, 3, 3264-3270.

[2] *Inorg. Chem.*, 2017, 56, 1041-1044.

[3] *ACS Sustainable Chem. Eng.*, 2018, 6, 16255-16266.

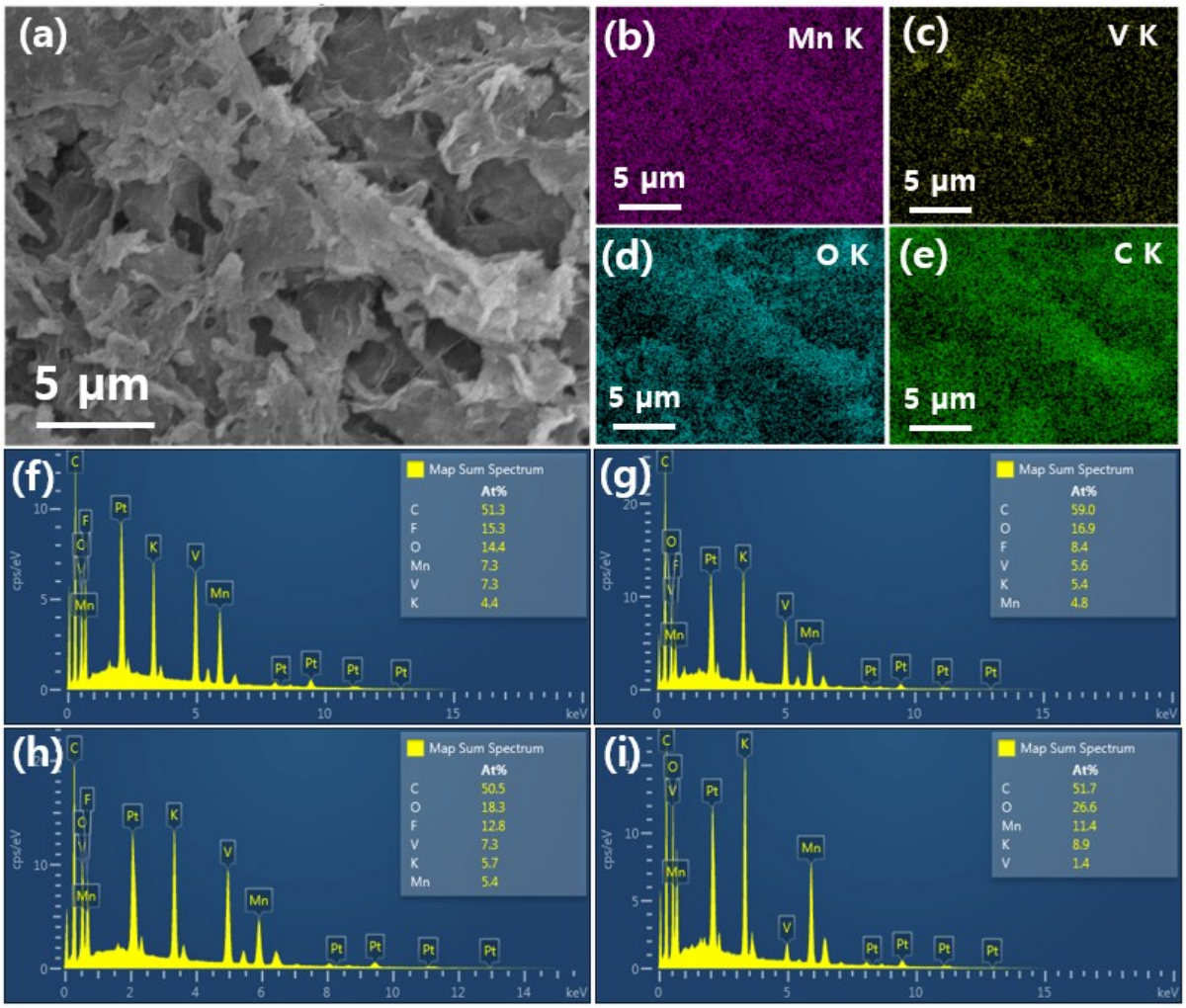

Fig. S7. (a) SEM image of MVO/G-20 after 1000 CV OER electrolysis and EDS mapping images of (b) Mn K, (c) V K, (d) O K, and (e) C K, respectively, and obtained EDS spectra for different areas (f-i).

"The SEM-EDS results show that although the distribution of Mn and V was similar (Fig. S7a-e†), the fraction of V was relatively low (Fig. S7f-i†) indicating that V dissolution occurred after 1000 CV cycles, which is similar to the dissolution of V^{4+} and V^{5+} components under KOH or NaOH solution in other V-containing compounds.[4-6]"

[4] *Angew. Chem. Int. Ed.*, 2017, 56, 3289-3293.

[5] *J. Mater. Chem. A*, 2019, 7, 21911-21917.

[6] *Nanoscale*, 2020, 12, 3803-3811.

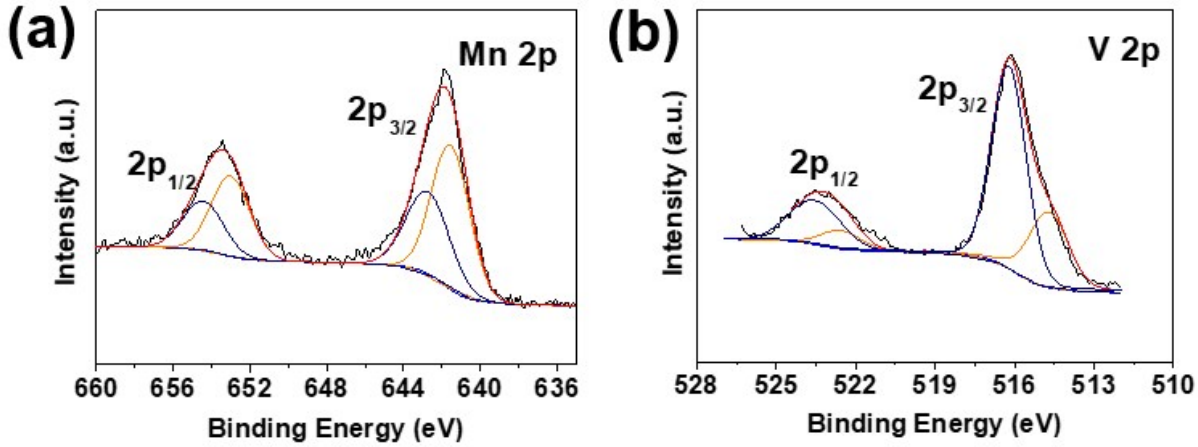

Fig. S8. XPS spectra of MVO/G-20 after 1000 CV OER electrolysis for (a) Mn 2p and (b) V 2p.

"The XPS spectra showed that the surface chemical states of MVO/G-20 underwent obvious changes (Fig. S8†). The Mn $2p_{3/2}$ spectrum was deconvoluted into two peaks located at 641.8 and 642.6 eV corresponding to Mn^{3+} and Mn^{4+} states, respectively,[7-8] indicating that pristine Mn^{2+} ion was oxidized after 1000 CV cycles (Fig. S8a†). On the other hand, V $2p_{3/2}$ spectrum was deconvoluted into two peaks located at 514.6 and 516.1 eV corresponding to V^{3+} and V^{4+} states, respectively,[9] indicating that pristine V^{5+} ion was mainly dissolved and reduced after 1000 CV cycles (Fig. S8b†). The dissolution of vanadium-ion species can affect catalytic activity[5,6] as it could lead to exposure of more OER active sites, valence change of other active species, and generation of oxygen vacancies, and further detailed mechanism study is required."

[7] *Am. Mineral.*, 1998, 83, 305-315.

[8] *Appl. Surf. Sci.*, 2011, 257, 2717-2730.

[9] *ChemSusChem*, 2019, 12, 240-251.